Structural, dynamical, electronic, and bonding properties of laser-heated silicon: An *ab initio* molecular-dynamics study

Pier Luigi Silvestrelli
Max-Planck-Institut für Festkörperforschung, Heisenbergstrasse 1, 70569 Stuttgart, Germany

Ali Alavi
Atomistic Simulation Group, School of Mathematics and Physics, The Queen's University, Belfast BT7 1NN, Northern Ireland, United Kingdom

Michele Parrinello
Max-Planck-Institut für Festkörperforschung, Heisenbergstrasse 1, 70569 Stuttgart, Germany

Daan Frenkel
FOM Institute for Atomic and Molecular Physics, Kruislaan 407, 1098 SJ, Amsterdam, The Netherlands
(Received 5 March 1997; revised manuscript received 21 April 1997)

The method of *ab initio* molecular dynamics, based on finite-temperature density-functional theory, is used to simulate laser heating of crystalline silicon. We found that a high concentration of excited electrons dramatically weakens the covalent bonding. As a result the system undergoes a melting transition to a metallic state. We studied several structural, dynamical, electronic, and bonding properties of this phase of silicon. In contrast to ordinary liquid silicon, this liquid is characterized by a high coordination number and a strong reduction of covalent-bonding effects. However this phase is transient. In fact, by strongly reducing the level of electronic excitation, liquid silicon reverts very rapidly to its usual properties. [S0163-1829(97)09631-8]

I. INTRODUCTION

The processes that occur in a semiconductor under intense laser irradiation have attracted considerable attention over the years because of the relevant technological importance and theoretical interest of the laser-annealing effect. In order to explain the observed phenomenology, contradictory explanations[1,2] were proposed. One of the first attempts to describe the microscopic mechanisms was the ''plasma-annealing'' (PA) model.[1] In this model it is suggested that a tetrahedral semiconducting material, subject to intense laser irradiation, can be directly driven into a disordered state long before the system has time to become vibrationally excited. In fact, laser irradiation induces electronic transitions from the bonding to antibonding states, thus depleting the bond charges. A high level of electronic excitation could severely weaken the interatomic bonds, so that room-temperature atomic motions can lead to the disordering of the lattice. The alternative explanation[2] was that direct energy transfer between the excited electrons and the ions leads to ordinary thermal melting (TM).

For laser pulses lasting 20 ps and longer, TM appears to be[2,3] the dominant mechanism. However, for very short irradiation times ($\sim$100 fs), recent time-resolved experiments strongly strengthened the PA model. In fact, with the use of ultrashort laser pulses, it is possible to excite the electronic states of a solid before appreciable energy is transferred to the lattice vibrational states. In particular, several groups[4] observed laser-induced melting of a GaAs crystal under high laser irradiation. Tom, Aumiller, and Brito-Cruz[5] reported a loss of cubic order in crystalline Si only 150 fs after an intense 100-fs optical pulse. Shank, Yen, and Hirlimann[6] observed melting of silicon on a time scale of less than 1 ps after a 90-fs pump pulse, as shown by optical reflectivity and second-harmonic generation. Sokolowski-Tinten, Bialkowski, and von der Linde[7] studied laser-induced ultrafast order-disorder transitions in Si and GaAs by means of femtosecond time-resolved linear and nonlinear optical spectroscopy. Similar phase transformations, induced by strong femtosecond laser pulses, were also observed[8] in InSb. In spite of this strong experimental evidence, a clear understanding of the processes that take place is still lacking.

Reasonable estimates[9] suggest that the relaxation time for the electrons, $\tau_{ee}\sim 10^{-14}$ s, is much shorter than the electron-ion relaxation time, $\tau_{eI}\sim 10^{-12}$ s. Therefore one can treat the subsystems of electrons and ions in a different way, by assuming that, after irradiation and for times smaller than τ_{eI}, the electron subsystem remains in internal equilibrium at the initial laser-induced temperature, which is different from that of the ions. Instead the ions are allowed to evolve freely. In order to describe this situation we used the *ab-initio* molecular-dynamics (MD) simulation technique introduced by Alavi *et al.*[10] This method is based on finite-temperature density-functional theory (DFT), and incorporates self-consistently the effects of thermal electronic excitations and fractionally occupied states. Thus it is particularly suited to describe the electronically hot subsystem. We find that, as a result of the large concentration of excited electrons, the effective ion-ion interactions are changed. This leads to the melting of the crystal and to the formation of a liquid metal (l'-Si) with properties different from those of ordinary liquid Si (l-Si). However, by reducing the electronic temperature to the average value of the ionic temperature of l'-Si, the system is found to recover the usual behavior of l-Si in a very

0163-1829/97/56(7)/3806(7)/$10.00 © 1997 The American Physical Society

short time. A short preliminary version of our results was presented elsewhere.[11]

The outline of the paper is as follows. In Sec. II we present our algorithm and provide computational details. In Sec. III the simulation of laser irradiation and the details of the observed melting process are described. Sec. IV contains the results of our study of structural, dynamical, electronic, and bonding properties of l'-Si. In Sec. V the effect of bond weakening, due to the presence of excited electrons, is illustrated by studying the equilibrium structure of three simple molecules, namely, SiH_4, Si_2H_6, and Si_2. Finally, our conclusions are presented in Sec. VI.

II. METHOD AND TECHNICAL DETAILS

Our *ab initio* MD simulation was performed at constant volume, by assuming the experimental density of crystalline Si at room temperature, namely $\rho = 2.329$ g cm^{-3} (Ref. 12). We used norm-conserving pseudopotentials[13] with s nonlocality only. The Γ point only was used to sample the Brillouin zone (BZ) of the MD supercell, containing $N=64$ atoms with periodic boundary conditions (PBC's) of the simple cubic type. The electronic orbitals were expanded in plane waves with a cutoff of 9.4 Ry.

Since we assumed that the electrons are in equilibrium at a temperature $T_{\rm el}$, their density $n(\mathbf{r})$ has to be computed by minimizing the electronic free energy $\mathcal{F}$. Following Ref. 10, we write

$$\mathcal{F} = \Omega + \mu N_e + E_{II}, \tag{1}$$

where

$$\Omega[n(\mathbf{r})] = -\frac{2}{\beta}\ln\det(1+e^{-\beta(\mathcal{H}-\mu)}) - \int d\mathbf{r}\, n(\mathbf{r}) \times\left(\frac{\phi(\mathbf{r})}{2} + \frac{\delta\Omega_{\rm xc}}{\delta n(\mathbf{r})}\right) + \Omega_{\rm xc}, \tag{2}$$

$\beta = 1/(k_B T_{\rm el})$ is the inverse electronic temperature, μ is the chemical potential, N_e is the total number of valence electrons, $\mathcal{H} = -\frac{1}{2}\nabla^2 + V(\mathbf{r})$ is the one electron Hamiltonian with the effective potential $V(\mathbf{r}) = \Sigma_I V_{\rm el}(\mathbf{r}-R_I) + \phi(\mathbf{r}) + \delta\Omega_{\rm xc}/\delta n(\mathbf{r})$, $\phi(\mathbf{r})$ is the Hartree potential of an electron gas of density $n(\mathbf{r})$, $\Omega_{\rm xc}$ the exchange-correlation energy in the local-density approximation (LDA), and E_{II} the classical Coulomb energy of the ions. The functional $\Omega_{\rm xc}$ is approximated by its $T_{\rm el}=0$ expression, since its finite-temperature corrections are negligible[14] at the temperatures and the electronic densities of our system. $\mathcal{F}$ reproduces the exact finite-temperature density of the Mermin functional,[15] and was optimized for each ionic configuration using a self-consistent diagonalization method.[10] In order to take the high level of electronic excitation into account, we computed 300 single-particle electronic states, that is, we included 172 extra states beyond the 128 needed for the calculation of the ground state. The electronic density is expressed in terms of the single-particle orbitals

$$n(\mathbf{r}) = \sum_i f_i |\psi_i(\mathbf{r})|^2, \tag{3}$$

where f_i are the Fermi-Dirac occupation numbers, $f_i = (e^{(E_i-\mu)/k_BT}+1)^{-1}$, and the ionic forces are calculated using the Hellmann-Feynman theorem. The ionic degrees of freedom were integrated using a time step of 25 a.u. ($\sim$0.6 fs). We are well aware that LDA underestimates[16] the energy gap and that, furthermore, use of the Γ point only of the supercell gives a poor representation of the density of states of the conduction band. However, the antibonding character of the conduction states is preserved and, at high levels of excitation, only the gross features of the conduction band are relevant, and these are well described by our approximation.

III. SIMULATION OF LASER IRRADIATION AND MELTING PROCESS

In the first part of the simulation the system was equilibrated, for 0.3 ps, at a temperature of 300 K, the Si ions being allowed to perform small oscillations around the sites of a perfect diamond lattice. In this phase the electronic temperature was kept equal to the average ionic temperature ($T_{\rm el}=300$ K), that is, the electrons were assumed to be in thermal equilibrium with the ions. After that, the effect of laser irradiation was simulated by suddenly increasing $T_{\rm el}$ to 25 000 K. This electronic temperature corresponds to a typical photon energy ($\sim$2.15 eV) of the laser radiation pulses used in experiments.[1,5] After irradiation we kept the electrons in this highly excited state, and we continued the MD simulation in the microcanonical ensemble. In the first 0.1 ps the silicon ions acquired a large amount of kinetic energy due to the fact that they were subject to interactions that were quite different from the ones operative at $T_{\rm el}=300$ K. Then the ionic temperature stabilized around a value of $\sim$1700 K, which is very close to the experimental melting point of Si (1680 K). In the following 0.3 ps we computed the averaged values of several properties of the laser-heated system. The instantaneous values of the ionic temperature $T_{\rm ion}(t)$, the free energy $\mathcal{F}(t)$, and the atomic mean-square displacement $R^2(t)$, are shown in Fig. 1. $T_{\rm ion}(t)$ is defined as

$$T_{\rm ion}(t) = \frac{M}{(3N-3)k_B}\sum_{I=1}^{N} v_I^2(t), \tag{4}$$

where k_B is the Boltzmann constant, M is the Si ion mass, and $v_I(t)$ the ionic velocity at time t, while $R^2(t)$ is given by

$$R^2(t) = \frac{1}{N}\sum_{I=1}^{N} [\mathbf{R}_I(t) - \mathbf{R}_I(0)]^2, \tag{5}$$

where $\mathbf{R}_I(t)$ denotes the coordinate of the Ith ion at time t. $T_{\rm ion}$ remains stable for about 60 fs, after which it rises monotonically to reach an equilibrium value of $\sim$1700 K. At this temperature the system behavior is highly diffusive. In fact $R^2(t)$ increases monotonically with an estimated diffusion coefficient of $D \sim 2.7\times10^{-4}$ cm^2 s^{-1}, a value comparable to the result (2.3×10^{-4} cm^2 s^{-1}) obtained in the *ab initio* MD simulation[17] of l-Si. Several conclusions can be drawn from the observation of Fig. 1. The system becomes disordered; however the hypothesis[1,4,5] that this happens while the lattice remains relatively cold can be rejected. Furthermore melting does not proceed via a mechanical instability due to phonon softening.[1,18] In fact, after irradiation, the ionic instantaneous

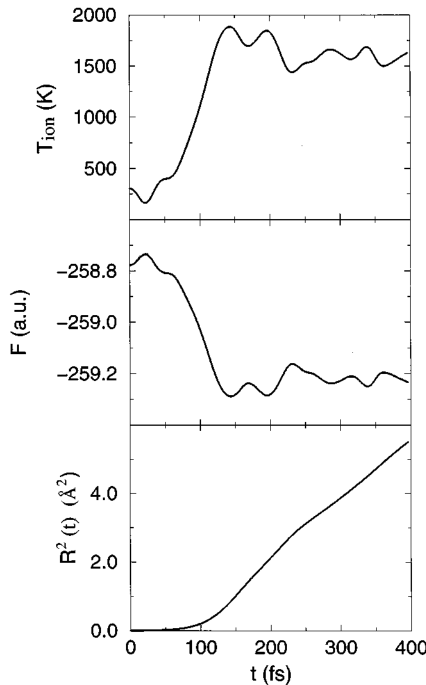

FIG. 1. Time dependence of the instantaneous values of the ionic temperature $T_{\mathrm{ion}}(t)$, the free energy $\mathcal{F}(t)$, and the atomic mean-square displacement $R^2(t)$, after laser irradiation.

temperature initially decreases, and the free energy increases. We estimated the effect of the distortions caused by phonons, calculating the free-energy functional of Eq. (1) for suitable, small atomic displacements from the equilibrium positions of the perfect diamond lattice. According to our calculation results, at $T_{\mathrm{el}}=25\,000$ K, the phonon modes are all positive, albeit somewhat softer (of the order of 10%) than in the equilibrium ($T_{\mathrm{el}}=300$ K) Si lattice. The same result has also been obtained using a smaller simulation supercell, containing eight Si atoms, and a more thorough sampling (64 k points) of the BZ. Melting therefore proceeds via a different mechanism. Laser irradiation changes the interatomic potential rather abruptly. Thus the system finds itself in a metastable region of phase space. After about 60 fs, under the action of the changed potential, it undergoes a collective transition to a different equilibrium state, which is an interesting liquid form of silicon (l'-Si), in order to lower its free energy. However this state of Si is only a transient. In fact, when the electrons decay to their ground state and the excess energy is dissipated, Si will revert to its usual thermodynamic behavior. We explicitly checked this by continuing the MD simulation with a much lower electronic temperature ($T_{\mathrm{el}}=1700$ K), approximately equal to the average ionic temperature of the liquid phase. In a very short time, on the order of 100 fs, the properties of the system (see Sec. IV) become very similar to those of l-Si, as observed in experiments and *ab initio* simulations.

We also performed a simulation of the laser-irradiated silicon crystal in which the electronic temperature was equal to $T_{\mathrm{el}}=15\,000$ K (~ 1.29 eV). Under these conditions the ions oscillated wildly around their equilibrium positions but the system did not melt, at least on the time scale of the simulation (~ 0.4 ps). However, since the atomic mean-square fluctuations were close to the critical value of Lindemann melting criterion, we believe that at this electronic temperature one should also observe melting in a long enough run. In simulations that use PBC's it is not infrequent to observe superheating of a perfect crystal. This is due to the finite simulation time and the absence of nucleation centers such as surfaces.

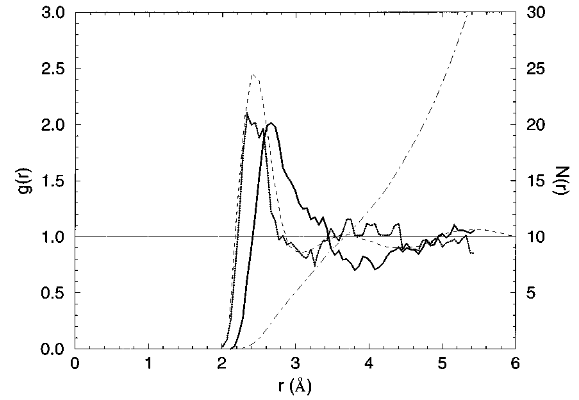

FIG. 2. Pair correlation function $g(r)$. Full line: MD simulation of l'-Si, at $T_{\mathrm{el}}=25\,000$ K; dotted line: continuation of the MD simulation at $T_{\mathrm{el}}=1700$ K; dashed line: experimental result (Ref. 19) for l-Si; dot-dashed line: coordination number $N(r)$ of l'-Si.

IV. PROPERTIES OF LASER-HEATED SILICON

A. Structural and dynamical properties

The laser-induced change in the interatomic potential is reflected in the form of the pair-correlation function $g(r)$ (Fig. 2) which, although somewhat noisy due to the short run, is clearly different from the same function of l-Si. In particular there is a remarkable shift in the position of the first peak which moves from the *ab initio* MD value[17,19] of 2.4–2.5 Å(experimental[20] 2.40 Å) for l-Si, to a larger value of ~ 2.7 Å. Furthermore the first peak, in l'-Si, is substantially lowered and broadened. Due to an ill-defined minimum after the first peak, it is difficult to define a coordination number. We estimate it to be between 11 and 13, that is, much larger than the value (6-7) of l-Si and approaching the high coordination of simple liquid metals. Analysis (see Fig. 3) of the distribution of the local coordination [the coordination shell being defined by $r_m=4.0$ Å, that is, around the first minimum of $g(r)$] indicates the presence of a broad distribution of local coordination, dominated by the values 12 and 13. However, bonding in l'-Si is rather complex, as reflected by the asymmetry in the first peak and the presence of a pronounced shoulder.

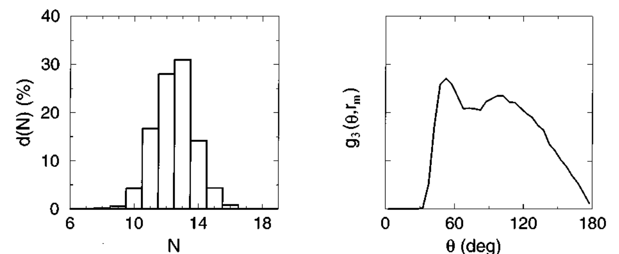

FIG. 3. Distribution $d(N)$ of local coordination (left panel) and bond-angle distribution function $g_3(\theta,r_m)$ (right panel) for l'-Si. The cutoff distance is equal to $r_m=4.0$ Å.

TABLE I. Si crystal in the diamond structure. Parameters of Murnaghan's equation of state, calculated at two different electronic temperatures. The experimental values, in parentheses, were measured (see Ref. 21) at 77 K.

T_{el}	V_0/V_{expt}	$P(V_{\mathrm{expt}})$ (kbar)	B_0 (Mbar)	B_0'
300 K	0.96	-44.2	1.26 (0.99)	4.0 (4.2)
25 000 K	1.18	115.5	0.45	4.8

In Fig. 2 we also report the pair-correlation function obtained by continuing, for 200 fs, the MD simulation at the reduced electronic temperature of $T_{\mathrm{el}}=1700$ K, a value approximately equal to the average ionic temperature reached by the system after laser irradiation. In this case the $g(r)$ function was computed by averaging over the MD configurations of the last 100 fs. Due to the limited number of sampled ionic configurations there is a relevant noise in the form of $g(r)$, however it clearly resembles the experimental pair-correlation function of l-Si. Moreover the coordination number is found to be 6–7, that is, just in the range of values appropriate for l-Si. This means that the l'-Si phase is only a transient state. In fact, as a consequence of a sudden decrease of the electronic excitation, the system returns very rapidly to the usual behavior of l-Si.

Additional information on the short-range order of l'-Si can be obtained from higher-order correlation functions, particularly by the bond-angle distribution function $g_3(\theta,r_m)$ which measures triplet correlations. Here θ indicates the angle between the two vectors that join a central particle with two neighbors at a distance smaller than r_m. Our $g_3(\theta,r_m)$, shown in Fig. 3, is rather broad with maxima centered at $\theta\sim52°$ and $\theta\sim97°$. It is similar to the $g_3(\theta,r_m)$ function obtained in MD simulations of l-Si (Ref. 17).

The effect of the high electronic excitation on the static structural properties of the Si crystal can be clearly understood by inspection of Table I and Fig. 4. The equilibrium volume V_0 and the bulk modulus B_0 and its pressure derivative B_0' at V_0 can be obtained from the calculated free energies $\mathcal{F}$ as a function of the volume. We computed $\mathcal{F}$ of the Si crystal in the diamond structure for some atomic volumes, at $T_{\mathrm{el}}=300$ K and at $T_{\mathrm{el}}=25\,000$ K. Then we have fitted our data to Murnaghan's equation of state[22]

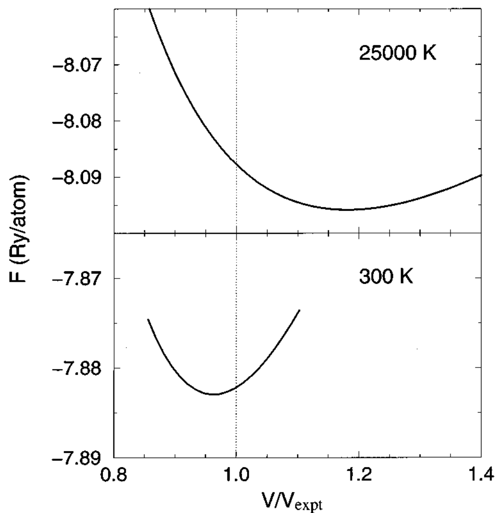

FIG. 4. Si crystal in the diamond structure. Free-energy curves as a function of the atomic volume (normalized to V_{expt}), computed by fitting the Murnaghan's equation of state, at $T_{\mathrm{el}}=300$ K (lower panel) and $T_{\mathrm{el}}=25\,000$ K (upper panel).

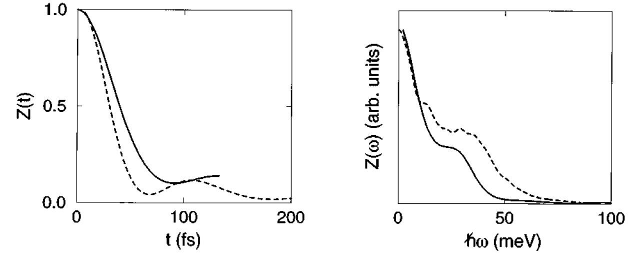

FIG. 5. Dynamical properties. Left panel: velocity autocorrelation function $Z(t)$. Right panel: the corresponding power spectrum $Z(\omega)$. Full line: MD simulation of l'-Si; dashed line: MD simulation of l-Si (Ref. 17).

$$\mathcal{F}(V)=\frac{B_0V}{B_0'}\left[\frac{(V_0/V)^{B_0'}}{B_0'-1}+1\right]+\text{const.} \tag{6}$$

At $T_{\mathrm{el}}=300$ K our fitted parameters are close enough to the experimental values. Notice that our computed equilibrium volume is slightly smaller than the experimental one, in such a way that at V_{expt} the system has a negative pressure. This fact is in agreement with the results of previous *ab initio* calculations[23] on semiconductors. The effect of increasing the electronic temperature to $T_{\mathrm{el}}=25\,000$ K is quite evident. In fact, at V_{expt}, the pressure of the system, with excited electrons, is large and positive. This is due to the fact that, as a consequence of the weakening of the covalent bonds, the distance between nearest-neighboring Si ions tend to increase so that the system, in the diamond structure, would be in equilibrium at a volume significantly larger than V_{expt}. Interestingly, we found that, at V_{expt}, the fcc structure, which is highly unfavored at $T_{\mathrm{el}}=300$ K, is instead significantly lower in free energy (~0.3 eV/atom) than the diamond structure as the electronic temperature is raised to $T_{\mathrm{el}}=25\,000$ K. Of course this behavior is in agreement with our previous analysis of the pair-correlation function, and confirms that the laser-heated system tends to transform to a more closed-packed structure.

The dynamical properties of l'-Si are also modified with respect to those of l-Si. As in l-Si (Ref. 17), our computed velocity autocorrelation function (Fig. 5)

$$Z(t)=\frac{\langle \mathbf{v}(0)\mathbf{v}(t)\rangle}{\langle \mathbf{v}(0)\mathbf{v}(0)\rangle} \tag{7}$$

is always positive, leading to the high value of the diffusion coefficient. However, the decay to zero of our $Z(t)$ appears to be slower than in l-Si. Obviously the opposite behavior is exhibited by the spectral density $Z(\omega)$, obtained by taking the Fourier transform of $Z(t)$. Nonetheless, as found in l-Si, our $Z(\omega)$ has a pronounced shoulder at the frequency of ~25 meV (Ref. 24).

B. Electronic properties

The metallic character of l'-Si is evident from looking at the electronic density of states $N(E)$ and the frequency-dependent electrical conductivity $\sigma(\omega)$. These quantities, which are shown in Fig. 2 of Ref. 11, appear to be very similar to those of l-Si (Ref. 17).

$N(E)$, which was calculated by averaging over 20 uncorrelated ionic configurations, displays a metallic character, as shown by the absence of a gap at the Fermi level. Our $N(E)$ appears somewhat ragged due to the shortness of the run, the limited energy resolution, and the use of the Γ-point only sampling of the BZ. In spite of these limitations, $N(E)$ is rather free-electron-like. We expect that these general features will not change with a more thorough **k**-point sampling and with a much longer run, the main effect of which should be simply to produce a smoother curve.[17,25]

$\sigma(\omega)$ was computed by averaging, again over 20 uncorrelated ionic configurations, the result of the Kubo-Greenwood formula[26]

$$\sigma(\omega,R_I)=\frac{2\pi e^2}{3m^2\omega}\frac{1}{V_b}\sum_{i,j}(f_i-f_j)|\langle\psi_i|\hat{p}|\psi_j\rangle|^2 \times\delta(E_j-E_i-\hbar\omega), \quad (8)$$

where e and m are the electronic charge and mass, V_b is the simulation box volume, $\hat{p}$ is the momentum operator, and ψ_i and E_i, are the electronic DFT eigenstates and eigenvalues, calculated for the ionic configuration $\{R_I\}$. Use of the Kubo-Greenwood formula in the present metastable situation (hot electrons, cold ions) is justified due to the assumption $\tau_{ee}\ll\tau_{eI}$. By extrapolating $\sigma(\omega)$ to zero frequency, we obtained a dc electrical conductivity $\sigma\sim 17.5\times 10^3\ \Omega^{-1}\ \mathrm{cm}^{-1}$, that is the same value calculated in the simulation[17] of l-Si, and close enough to the experimental value $(12.4\times 10^3\ \Omega^{-1}\ \mathrm{cm}^{-1})$ measured[27] in l-Si. As in l-Si (Refs. 17 and 28), our computed $\sigma(\omega)$ shows a Drude-like behavior. By fitting a Drude curve

$$\sigma(\omega)=\frac{\sigma(0)}{1+\omega^2\tau^2} \quad (9)$$

to our data in the range (1.2–3.1 eV) of the photon energies investigated experimentally in l-Si, we estimate a relaxation time $\tau^{-1}\simeq 2.15$ eV. This value is comparable to the relaxation time measured experimentally[28] ($\tau^{-1}\simeq 2.99$ eV), and computed by simulation[17] ($\tau^{-1}\simeq 2.93$ eV) in l-Si.

The average concentration of photoexcited electron-hole pairs n_{eh}, at $T_{el}=25\,000$ K can be readily estimated by means of the Fermi-Dirac occupation numbers. In fact,

$$n_{eh}=\frac{2}{V_b}\sum_{i>N_e/2}\langle f_i\rangle, \quad (10)$$

where brackets indicate an average performed over the MD configurations. We obtain $n_{eh}=3.4\times 10^{22}\ \mathrm{cm}^{-3}$, corresponding to a fraction of about 17% of the total number of valence electrons. This value is in reasonable agreement with experimental estimates[7] based on the density of absorbed optical energy.

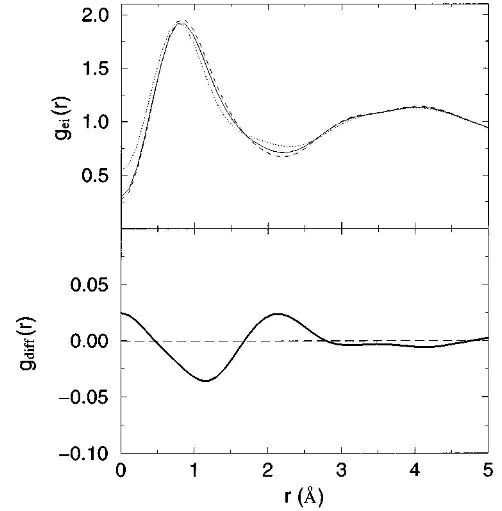

FIG. 6. Electron-ion pair-correlation functions g_{ei} in the diamond lattice configuration. Upper panel: g_{ei}(25 000K) (full line), g_{ei}(300K) (dashed line), g_{ei} produced by the superposition of atomic charge densities (dotted line). Lower panel: $g_{diff}=g_{ei}(25\,000\mathrm{K})-g_{ei}(300\mathrm{K})$.

C. Bonding properties

In order to clarify the effect of the high electronic temperature, we considered a fixed ionic configuration, with the ions located at the equilibrium positions of the perfect diamond lattice, and computed the different electronic charge distributions obtained by minimizing $\mathcal{F}$ at different electronic temperatures. Figure 5 of Ref. 11 shows contour plots of $\Delta n(\mathbf{r})$, defined as the difference between the charge density computed at $T_{el}=25\,000$ K and that computed at $T_{el}=300$ K. It is evident that, at $T_{el}=25\,000$ K, a significant amount of electronic charge, which can be estimated of the order of 0.1 electrons per atom, is removed from the covalent bond.

As in Ref. 29 we computed the electron-ion pair-correlation function g_{ei}, which describes the correlation between the local density of the electrons and the local density of the ions, according to

$$g_{ei}(r)=\frac{1}{4\pi r^2 n_0 N}\sum_{I=1}^{N}\int d\mathbf{r}' n(\mathbf{r}')\,\delta(|\mathbf{r}'-\mathbf{R}_I|-r), \quad (11)$$

where n_0 is the averaged density of electrons. In our simulations we only considered interactions between the valence electrons and the Si^{4+} ions, therefore $n(\mathbf{r})$ is the pseudocharge instead of the real charge density. As a consequence, the actual shape of the electronic charge density at the atomic cores cannot be accurately given by our calculation. This inaccuracy, however, concerns a small region around the atomic nuclei and has no effect on the charge density at larger distances, namely, in the region interesting for cohesive properties. In Fig. 6 we report the g_{ei} functions obtained, at $T_{el}=300$ K and at $T_{el}=25\,000$ K, again with the ions located in the diamond lattice. Although the spherical average implicit in the calculation of g_{ei} does not allow it to give a precise description in terms of directional bonds, the clear

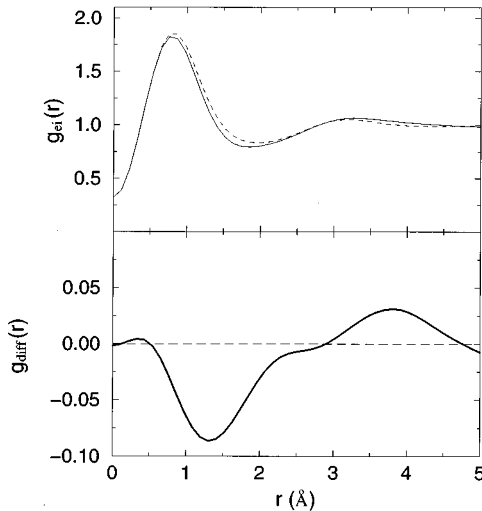

FIG. 7. Electron-ion pair correlation functions g_{ei} obtained by averaging over many ionic configurations of the MD simulation. Upper panel: g_{ei}(25 000K) (full line), g_{ei}(1700K) (dashed line). Lower panel: $g_{diff}=g_{ei}(25\ 000\text{K})-g_{ei}(1700\text{K})$.

difference between the g_{ei}'s computed at different electronic temperatures is evident. In the same figure we also plot the $g_{ei}(r)$ function corresponding to a superposition of atomic charge densities. As can be seen, the $g_{ei}(r)$ at $T_{el}=25\ 000$ K appears to be intermediate between the same function at $T_{el}=300$ K and the $g_{ei}(r)$ produced by the superposition of atomic charge densities. The analysis of $g_{diff}=g_{ei}$ (25 000 K) $-g_{ei}$ (300 K) is particularly illuminating. In fact a strong depletion of electronic charge, at a distance of ~1.2 Å from each Si ion, is evident. Since 1.2 Å is just equal to half the covalent bond length in crystalline Si, this means that in the electronically excited system the strength of the covalent bond is severely reduced.

In Fig. 7 we plot $g_{ei}(r)$, obtained by averaging over many ionic configurations of our MD simulation with excited electrons ($T_{el}=25\ 000$ K), together with the same function calculated by continuing the simulation at $T_{el}=1700$ K. The behavior is similar to that observed in the previous analysis of the diamond lattice configuration. In fact, the curve representing the difference between the two pair-correlation functions clearly indicates that the high level of electronic excitation characteristic of l'-Si considerably reduces the effects of the covalent bonds which are still effective in l-Si.[17]

V. BOND WEAKENING IN MOLECULES

To give further support to the concept of weakening of the covalent bond, due to the presence of excited electrons, we also determined the effect of the high electronic excitation ($T_{el}=25\ 000$ K) on the equilibrium structure of three simple molecules, namely SiH_4 (silane), Si_2H_6 (disilane), and Si_2. The electronic orbitals were expanded in plane waves with an energy cutoff of 14 Ry for SiH_4, and of 10 Ry for Si_2H_6 and Si_2. The size of the supercell was chosen to be sufficiently large to make dispersion effects and interactions between different images of the molecules negligible. The electron-ion interactions were modeled using a standard norm-conserving pseudopotential,[13] with s nonlocality, for Si, and a local norm-conserving pseudopotential[30] for H. A standard steepest-descent method was used to minimize the free-energy functional $\mathcal{F}$ and to determine the equilibrium structures of the molecules.

TABLE II. Bond lengths d (in Å) at two different electronic temperatures.

	Si_2	SiH_4	Si_2H_6	
	d(Si-Si)	d(Si-H)	d(Si-Si)	d(Si-H)
25 000 K	broken	1.68	broken	1.73
300 K	2.24	1.53	2.35	1.54
Other simulations	2.20 [a]	1.52 [b]		
Experiment	2.24 [c]	1.48 [d]	2.33 [d]	1.49 [d]

[a]Reference 31.
[b]Reference 32.
[c]Reference 33.
[d]Reference 34.

In Table II we report the equilibrium bond lengths, computed at $T_{el}=300$ K and $T_{el}=25\ 000$ K, together with the results obtained by other *ab initio* simulations performed assuming zero electronic temperature, and with the corresponding experimental data. Our results, at $T_{el}=300$ K, are very close to the values computed in previous simulations and in experiments; however, increasing the electronic temperature to $T_{el}=25\ 000$ K, the molecular structure dramatically changes. In fact, in SiH_4 the presence of the excited electrons makes the Si-H bond length significantly (~ 10 %) longer. In Si_2H_6 the Si-H bond length is also increased considerably (~ 12 %), while the Si-Si bond is completely broken. The same is true for the Si_2 molecule, which is unstable at $T_{el}=25\ 000$ K.

VI. CONCLUSIONS

In conclusion, we have presented the results of an *ab initio* MD simulation of laser-heated Si. Admittedly, our simulation is a rather simplified modeling of the experiments. However we think that it captures the essential features of the phenomenon. Basically, the presence of a large concentration of excited electrons weakens the covalent bonds of the crystal and changes the interatomic forces, so that under the action of this modified interaction the system melts. In some sense our picture of the melting process is intermediate between the PA and TM models. As in PA, melting is triggered by a weakening of the covalent bonds, however the temperature of the ions is increased as in TM, albeit via a mechanism rather different from that of a direct transfer of energy from electrons to ions.

A detailed study of structural, dynamical, electronic, and bonding properties showed that the liquid, obtained by laser heating Si, has properties remarkably different from those of l-Si. In particular it is characterized by a high coordination number and a severe reduction of covalent bonding effects. However, this state of Si is only a transient phase, characteristic of the high level of electronic excitation reached by

means of laser irradiation. In fact, by reducing the electronic temperature to 1700 K, the system very rapidly assumes properties of the ordinary l-Si. The effect of bond weakening, due to the presence of a high concentration of excited electrons, has also been discussed by studying the equilibrium structures of small molecules.

ACKNOWLEDGMENTS

Part of this work was done while P. L. S. was at the FOM Institute and was supported by the Nederlandse Organisatie voor Wetenschappelijk Onderzoek (NWO). Computer time on the CRAY-C98/4256 at SARA was made available by the Stichting Nationale Computer Faciliteiten (NCF).

[1] J. A. Van Vechten, R. Tsu, F. W. Saris, and D. Hoonhout, Phys. Lett. **74A**, 417 (1979); **74A**, 422 (1979); J. A. Van Vechten, J. Phys. Colloq. **41**, C4-15 (1980); J. A. Van Vechten, in *Laser and Electron-Beam Interactions with Solids*, edited by B. R. Appleton and G. K. Celler (North-Holland, New York, 1981), Vol. 4.

[2] *Pulsed Laser Processing of Semiconductors*, edited by R. F. Wood, C. W. White, and R. T. Young (Academic, Orlando, 1984), Vol. 23, and references quoted therein.

[3] *Resonances—A Volume in Honor of the 70th Birthday of Nicolaas Bloembergen*, edited by M. D. Levenson, E. Mazur, P. S. Pershan, and Y. R. Shen (World Scientific, Singapore, 1990), and references quoted therein.

[4] S. V. Govorkov, I. L. Shumay, W. Rudolph, and T. Schroder, Opt. Lett. **16**, 1013 (1991); P. Saeta, J.-K. Wang, Y. Siegal, N. Bloembergen, and E. Mazur, Phys. Rev. Lett. **67**, 1023 (1991); K. Sokolowski-Tinten, H. Schulz, J. Bialkowski, and D. von der Linde, Appl. Phys. A **53**, 227 (1991).

[5] H. W. K. Tom, G. D. Aumiller, and C. H. Brito-Cruz, Phys. Rev. Lett. **60**, 1438 (1988).

[6] C. V. Shank, R. Yen, and C. Hirlimann, Phys. Rev. Lett. **50**, 454 (1983); **51**, 900 (1983).

[7] K. Sokolowski-Tinten, J. Bialkowski, and D. von der Linde, Phys. Rev. B **51**, 14 186 (1995).

[8] I. L. Shumay and U. Höfer, Phys. Rev. B **53**, 15 878 (1996).

[9] D. Agassi, J. Appl. Phys. **55**, 4376 (1984).

[10] A. Alavi, J. Kohanoff, M. Parrinello, and D. Frenkel, Phys. Rev. Lett. **73**, 2599 (1994).

[11] P. L. Silvestrelli, A. Alavi, M. Parrinello, and D. Frenkel, Phys. Rev. Lett. **77**, 3149 (1996).

[12] Y. Tatsumi and H. Ohsaki, *Properties of Silicon* (INSPEC, London), 1988, p. 3.

[13] G. B. Bachelet, D. R. Hamann, and M. Schlüter, Phys. Rev. B **26**, 4199 (1982); L. Kleinman and D. M. Bylander, Phys. Rev. Lett. **48**, 1425 (1982).

[14] F. Perrot and M. W. C. Dharma-wardana, Phys. Rev. A **30**, 2619 (1984); D. G. Kanhere, P. V. Panat, A. K. Rajagopal, and J. Callaway, *ibid.* **33**, 490 (1986).

[15] N. D. Mermin, Phys. Rev. **137**, A1441 (1965).

[16] See, for instance, R. M. Dreizler and E. K. U. Gross, *Density Functional Theory* (Springer, Berlin, 1990), p. 145, and references quoted therein.

[17] I. Štich, R. Car, and M. Parrinello, Phys. Rev. Lett. **63**, 2240 (1989); Phys. Rev. B **44**, 4262 (1991).

[18] M. Combescot and J. Bok, Phys. Rev. Lett. **48**, 1413 (1982); R. Biswas and V. Ambegaokar, Phys. Rev. B **26**, 1980 (1982); P. Stampfli and K. H. Bennemann, *ibid.* **42**, 7163 (1990); **46**, 10 686 (1992); **49**, 7299 (1994).

[19] I. Štich, M. Parrinello, and J. M. Holender, Phys. Rev. Lett. **76**, 2077 (1996).

[20] Y. Waseda and K. Suzuki, Z. Phys. B **20**, 339 (1975); J. P. Gabathuler and S. Steeb, Z. Naturforsch. A **34A**, 1314 (1979).

[21] H. J. McSkimin, J. Appl. Phys. **24**, 988 (1953); H. J. McSkimin and P. Andreatch, Jr., *ibid.* **34**, 651 (1963); **35**, 2161 (1964).

[22] F. D. Murnaghan, Proc. Natl. Acad. Sci. USA **30**, 244 (1944).

[23] V. Fiorentini, Phys. Rev. B **46**, 2086 (1992).

[24] We have discovered a trivial error in the calculation of $Z(\omega)$ reported in Ref. 11. The correct $Z(\omega)$ is the one present here. The conclusions of Ref. 11 are not affected by this error.

[25] W. Jank and J. Hafner, Phys. Rev. B **41**, 1497 (1990).

[26] E. N. Economou, *Green's Functions in Quantum Physics*, edited by M. Cardona, P. Fulde, and H.-J. Queisser, Springer Series in Solid State Sciences Vol. 7 (Springer, Berlin, 1983), p. 152ff.

[27] H. S. Schnyders and J. B. Van Zytveld, J. Phys. Condens. Matter **8**, 10 875 (1996).

[28] K. M. Shvarev, B. A. Baum, and P. V. Geld, Fiz. Tverd. Tela (Leningrad) **16**, 3246 (1974) [Sov. Phys. Solid State **16** 2111 (1975)].

[29] G. A. de Wijs, G. Pastore, A. Selloni, and W. van der Lugt, Phys. Rev. Lett. **75**, 4480 (1995).

[30] The local potential for H was derived by P. Giannozzi (unpublished), and its description can be found in F. Gygi, Phys. Rev. B **48**, 11 692 (1993).

[31] N. Binggeli and J. R. Chelikowsky, Phys. Rev. B **50**, 11 764 (1994).

[32] G. Onida and W. Andreoni, Chem. Phys. Lett. **243**, 183 (1995).

[33] D. E. Milligan and M. E. Jacox, J. Chem. Phys. **52**, 2594 (1970), and references therein.

[34] J. H. Callomon, E. Hirota, K. Kuchitsu, W. J. Lafferty, A. G. Maki, and C. S. Pote, in *Structure Data of Free Polyatomic Molecules*, edited by K.-H. Hellwege and A. M. Hellwege, Landolt-Börnstein, New Series, Group 2, Vol. 7 (Springer, Berlin, 1976).